

# Design and Synthesis of “Dumb-bell” and “Triangular” Inorganic–Organic Hybrid Nanopolyoxometalate Clusters and Their Characterisation through ESI-MS Analyses

Chullikkattil P. Pradeep,<sup>[a, b]</sup> Feng-Yan Li,<sup>[a, c]</sup> Claire Lydon,<sup>[a]</sup> Haralampos N. Miras,<sup>[a]</sup> De-Liang Long,<sup>[a]</sup> Lin Xu,<sup>[c]</sup> and Leroy Cronin\*<sup>[a]</sup>

**Abstract:** A series of tris(hydroxymethyl)aminomethane (TRIS)-based linear (bis(TRIS)) and triangular (tris(TRIS)) ligands has been synthesised and were covalently attached to the Wells–Dawson type cluster  $[P_2V_3W_{15}O_{62}]^{9-}$  to generate a series of nanometer-sized inorganic–organic hybrid polyoxometalate clusters. These huge hybrids, with a molecular mass similar to that of small proteins in the range of  $\approx 10$ –16 kDa, were unambiguously characterised by using high-resolution ESI-MS. The ESI-MS spectra of these compounds revealed, in negative

ion mode, a characteristic pattern showing distinct groups of peaks corresponding to different anionic charge states ranging from  $3^-$  to  $8^-$  for the hybrids. Each peak in these individual groups could be unambiguously assigned to the corresponding hybrid cluster anion with varying combinations of tetrabutylammonium (TBA)

and other cations. This study therefore highlights the prowess of the high-resolution ESI-MS for the unambiguous characterisation of large, nanoscale, inorganic–organic hybrid clusters that have huge mass, of the order of 10–16 kDa. Also, the designed synthesis of these compounds points to the fact that we were able to achieve a great deal of structural pre-design in the synthesis of these inorganic–organic hybrid polyoxometalates (POMs) by means of a ligand design route, which is often not possible in traditional “one-pot” POM synthesis.

**Keywords:** mass spectrometry · nanostructures · organic–inorganic hybrid composites · polyoxometalates · tungsten

## Introduction

Polyoxometalates (POMs) are an important class of inorganic compounds containing anionic metal oxide clusters of Mo, W, V and Nb, with interesting structural, physical and chemical properties.<sup>[1,2]</sup> One way of expanding the horizons of POM chemistry is through the development of inorganic–organic hybrids by combining POM clusters with various organic functionalities.<sup>[3]</sup> For instance the covalent binding of organic groups onto POM clusters is an important synthetic strategy towards functional hybrids, as the covalent functionalisation often allows synergistic interaction between or-

ganic units and inorganic clusters.<sup>[4]</sup> This means that covalent functionalisation could also lead to the development of POM hybrids with pre-designed topologies.<sup>[5]</sup> This structural pre-design is often not possible in traditional “one-pot” POM synthesis.<sup>[1]</sup>

Thus far, the majority of the inorganic–organic hybrid POMs reported in recent years are based on smaller cluster types, such as Lindqvist, Keggin and Anderson type clusters and/or their derivatives.<sup>[6]</sup> However, some of the recent attempts in this field are focussing on larger clusters, such as Wells–Dawson type clusters, which are more redox and catalytically active compared to smaller cluster types.<sup>[7–12]</sup> For example, the Wells–Dawson type clusters have the capability of accepting a number of electrons reversibly without cluster disintegration.<sup>[13]</sup> Nevertheless, compared to hybrids based on smaller cluster types, reports on Wells–Dawson cluster based hybrids are limited in the literature; one possible reason for this could be the difficulties associated with the characterisation of such huge hybrids. One major problem often faced in the characterisation of large POM hybrids is the difficulty in getting good quality crystals suitable for single-crystal X-ray analysis. For example, it is observed that POMs with a large number of organic cations, such as tetrabutylammonium (TBA), often do not form good quality crystals and even if they do, the crystals tend to crack immediately due to solvent loss or are poorly diffracting due to disorder associated with the many charge balancing cat-

[a] Dr. C. P. Pradeep, Dr. F.-Y. Li, C. Lydon, Dr. H. N. Miras, Dr. D.-L. Long, Prof. Dr. L. Cronin  
WestCHEM, Department of Chemistry  
The University of Glasgow, G12 8QQ (UK)  
Fax: (+44) 141-330-4888  
E-mail: L.Cronin@chem.gla.ac.uk

[b] Dr. C. P. Pradeep  
Present Address: School of Basic Sciences  
Indian Institute of Technology—Mandi  
Mandi 175 001, Himachal Pradesh (India)

[c] Dr. F.-Y. Li, Prof. Dr. L. Xu  
Key Laboratory of Polyoxometalate Science of Ministry of Education  
Department of Chemistry, Northeast Normal University  
Changchun, Jilin (P. R. China)

Supporting information for this article is available on the WWW under <http://dx.doi.org/10.1002/chem.201100257>.

ions.<sup>[14]</sup> On the other hand, it is generally agreed that the traditional solution characterisation techniques such as NMR spectroscopy, polarography, optical spectrophotometry and so forth are of limited application in the case of polyoxometalates with large size and high symmetry. In this context, there is a need for developing alternative characterisation techniques that can be reliably employed for a wide range of POM clusters, especially hybrid POMs that have huge masses, for example, reaching that of proteins.

Electrospray ionisation mass spectrometry (ESI-MS) is a successful technique for the characterisation of very large molecules of biological and pharmaceutical importance, and also for the characterisation of large supramolecular systems as well as coordination compounds.<sup>[15,16]</sup> For instance it has been found that ESI-MS could be a valuable tool in the analysis of polyoxometalates dissolved in organic or aqueous-organic solvents, as it involves a soft ionisation technique with respect to FAB MS, and serves to transfer/desorb ions from solution to the gas phase with minimal fragmentation along the ion path.<sup>[16]</sup> Following the pioneering works of early researchers in this area,<sup>[17]</sup> we have extensively utilised cryospray and electrospray ionisation MS techniques for the characterisation and elucidation of cluster transformation mechanisms in POM chemistry.<sup>[18]</sup> However, in order to establish high-resolution ESI-MS as a reliable characterisation technique in POM chemistry, more studies are needed covering a wide variety of compounds, especially hybrid POMs that have different size and mass ranges.

In this paper, we report the synthesis of a series of nanometer-sized hybrid POMs based on Wells–Dawson type cluster  $[P_2V_3W_{15}O_{62}]^{9-}$  that have masses of the order of 10–16 kDa, and their unambiguous characterisation using the ESI-MS technique. These “dumb-bell”- and “triangular”-shaped inorganic–organic hybrids are developed from tris(hydroxymethyl)aminomethane (TRIS)-based linear (bis(TRIS)) and “triangular” (tris(TRIS)) ligands and contain tetrabutylammonium (TBA) as the major counterion. Inorganic–organic hybrids containing one as well as four  $[P_2V_3W_{15}O_{62}]^{9-}$  units have been reported by groups of Hill and Hasenknopf.<sup>[7,10]</sup> The hybrids reported in the present paper containing two and/or three  $[P_2V_3W_{15}O_{62}]^{9-}$  cluster units are therefore, complementary to the above studies and are logical extension of our own previous report of “dumb-bell”-shaped hybrids containing two such units.<sup>[9]</sup> The main interest in  $[P_2V_3W_{15}O_{62}]^{9-}$ -based “dumb-bell”-type hybrids lies in their amphiphilic properties such as surfactant-like self-assembly behaviour in solutions leading to vesicle formation.<sup>[9]</sup> Although, this paper concentrates mainly on the synthesis and ESI-MS characterisation of some new  $[P_2V_3W_{15}O_{62}]^{9-}$ -based hybrids, detailed studies have shown that some of these compounds exhibits interesting self-assembly behaviour in solution, as expected.<sup>[19]</sup>

## Results and Discussion

**Synthesis and spectroscopic characterisation:** Tris(hydroxymethyl)aminomethane (TRIS) is an important linker molecule in POM chemistry, capable of binding an organic functionality at one end and a particular POM cluster at the other.<sup>[9,20,21]</sup> This bifunctional property of TRIS has led to the development of a number of TRIS-functionalised hybrid POMs, the majority of which are based on the Anderson type cluster. For example, Hasenknopf et al. have reported a series of TRIS-functionalised Mn-Anderson cluster hybrids in connection with light-harvesting and gel-formation properties.<sup>[21]</sup> Studies from our group have shown that TRIS-functionalised Mn-Anderson clusters can form interesting framework materials in the solid state and can exhibit surfactant type behaviour in solution, depending on the organic groups attached.<sup>[22]</sup> Also, asymmetric functionalisation of Mn-Anderson clusters, that is, attaching two different TRIS functionalities onto either side of the disc-shaped Anderson cluster, has also been achieved by our group, which ultimately led to the development of surface-grafted functionalised POMs, capable of exhibiting cell-adhesion properties.<sup>[23]</sup> TRIS-grafted  $[P_2V_3W_{15}O_{62}]^{9-}$  clusters have been reported by Hill et al., followed by a report on “super-POMs” containing four  $[P_2V_3W_{15}O_{62}]^{9-}$  units by the same group.<sup>[7]</sup> Some of these  $[P_2V_3W_{15}O_{62}]^{9-}$ -based hybrids are shown to exhibit catalytic properties towards peroxide oxidations of tetrahydrothiophene. Recently, TRIS-grafted  $[P_2V_3W_{15}O_{62}]^{9-}$  cluster hybrids have been utilised in the development of POM-polymer hybrids<sup>[11]</sup> as well as hybrid gels.<sup>[12]</sup> Studies from our group have shown that the self-assembly of  $[P_2V_3W_{15}O_{62}]^{9-}$  cluster in solutions and gas phase can be controlled by grafting TRIS derivatives with different hydrogen-bonding functionalities  $-NO_2$ ,  $-NH_2$  and  $-CH_3$ . ESI-MS studies on such hybrids could detect hydrogen-bonded higher aggregates formed in solution and in gas phase.<sup>[8]</sup> In a recent study, we have also shown that the  $[P_2V_3W_{15}O_{62}]^{9-}$  cluster could be used for the development of hybrids with amphiphilic properties. For example, “dumb-bell”-shaped hybrids, developed by connecting two  $[P_2V_3W_{15}O_{62}]^{9-}$  clusters together by using bis(TRIS) linkers, are shown to exhibit interesting self-assembly behaviour in solution leading to the formation of vesicles having dimensions of the order of 100 nm.<sup>[9]</sup> The solution characterisation of such “dumb-bell” clusters by ESI-MS analyses revealed that such large nanoclusters exhibit clear ESI-MS spectra consisting of groups of peaks corresponding to differently charged cluster anions, see Figure 1. This led us to explore this class of compounds further by varying the bis(TRIS) linker ligands and also by extending this class of compounds further by developing tris(TRIS) linker ligands.

In the present study, we have synthesised a series of bis(TRIS) and tris(TRIS) polyol ligands  $L^1$ – $L^6$  (shown here). The syntheses of bis(TRIS) ligands  $L^1$ – $L^3$  were achieved by using reported procedures,<sup>[24,25]</sup> involving the condensation of tris(hydroxymethyl)aminomethane with appropriate di- or tri-carboxylic acid esters in methanol at reflux tempera-

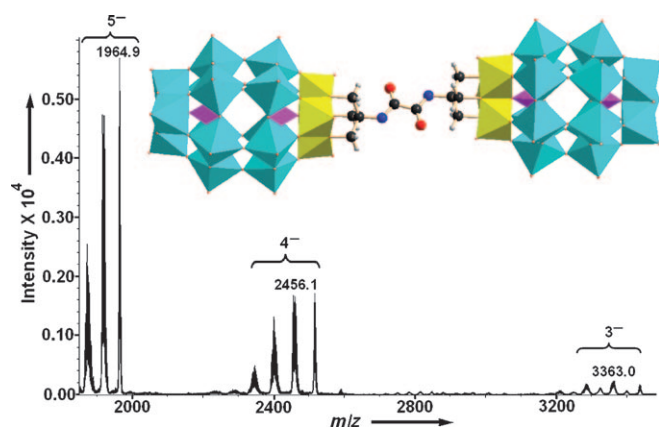
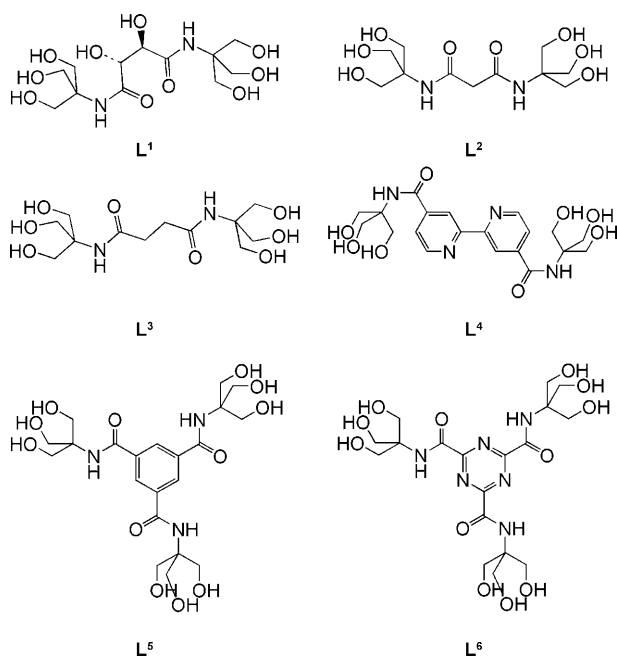


Figure 1. X-ray crystal structure as well as the ESI-MS spectrum of the hybrid polyoxometalate anion  $[\{P_2V_3W_{15}O_{59}(OCH_2)_3CNHCO\}_2]^{12-}$ .<sup>[9]</sup> W: cyan; V: yellow; P: purple; C: black; N: blue; O: red. This colour scheme is continued in the diagrammatic non-X-ray pictures in Figure 2–6.



tures. The synthesis of bipyridine based bis(TRIS) ligand **L**<sup>4</sup> and the tris(TRIS) ligands **L**<sup>5</sup> and **L**<sup>6</sup> were achieved employing the same synthetic procedure as that of **L**<sup>1</sup>–**L**<sup>3</sup>, starting from corresponding di- or tri- carboxylic acid esters.

Organic molecules containing the TRIS triol moiety are useful in diverse areas. In general, non-ionic polyol derivatives such as tris(hydroxymethyl)amidomethane derivatives are useful as sugar macronutrient substitutes, employed in the formulation of low-calorie food products.<sup>[24]</sup> Molecules containing TRIS tripodal alcohol moieties have been used as ligands in the synthesis of single-molecule magnetic clusters.<sup>[26]</sup> The compounds **L**<sup>5</sup> and **L**<sup>6</sup>, containing three TRIS moieties arranged around an aromatic platform, could be synthetically important to develop highly branched ligands, since such moieties may be used to anchor multiples of dendrons in the production of arborol dendrimers.<sup>[27]</sup> The re-

ported synthetic approaches for such molecules so far involved the use of peptide coupling agents such as EEDQ, or the use of activated aromatic carboxylic acid cores, which necessitates the protection of TRIS moiety prior to amide bond formation. However, the synthetic procedure reported in this paper represents a relatively simple and straight forward approach for such compounds.

The Wells–Dawson based hybrid clusters  $TBA_{10}H_2[\{P_2V_3W_{15}O_{59}(OCH_2)_3CNHCO\}_2(CHOH)_2]$  (**1**),  $TBA_{10}H_2[\{P_2V_3W_{15}O_{59}(OCH_2)_3CNHCO\}_2CH_2]$  (**2**),  $TBA_{10}H_2[\{P_2V_3W_{15}O_{59}(OCH_2)_3CNHCO\}_2(CH_2)_2]$  (**3**),  $TBA_{10}H_2[\{P_2V_3W_{15}O_{59}(OCH_2)_3CNHCO\}_2(C_3H_3N)_2]$  (**4**),  $TBA_{15}H_3[\{P_2V_3W_{15}O_{59}(OCH_2)_3CNHCO\}_3(C_6H_5)_3]$  (**5**) and  $TBA_{15}H_3[\{P_2V_3W_{15}O_{59}(OCH_2)_3CNHCO\}_3(C_6N_3)_3]$  (**6**) were synthesised in good yields by refluxing  $TBA_3H_4[P_2V_3W_{15}O_{62}]$  with **L**<sup>1</sup>–**L**<sup>6</sup>, respectively, in dry acetonitrile. The compounds thus obtained were characterised by elemental analyses, and IR and NMR spectroscopic techniques. The analytical data revealed that these hybrids contain V<sub>3</sub>-capped Wells–Dawson type clusters linked together by bis(TRIS)/tris-(TRIS) ligands as expected. Initial investigations into the thermal stability of compounds **1**–**6** were carried out using thermogravimetric analyses (TGA). The TGA profiles of these hybrids were similar and showed that they are thermally stable up to  $\approx 200^\circ\text{C}$ . At temperatures above  $200^\circ\text{C}$ , the hybrids start to decompose, most probably due to the loss of TRIS ligands and TBA counterions. The decomposition continues up until  $\approx 500^\circ\text{C}$  at which point a weight loss of approximately 27% is observed, and this corresponds to the loss of the organic ligand and TBA cations (see Supporting Information). The TGA profiles of compounds **1**–**6** are comparable to those of similar hybrid compounds reported before.<sup>[9]</sup> The electrochemical studies of compounds **1**–**6** revealed that their redox behaviours are also quite comparable to that of their parent hybrid cluster  $[H_2NC(CH_2O)_3P_2V_3W_{15}O_{59}]^{6-}$ , see Supporting Information for further details.

#### ESI-MS analyses of compounds **1**–**6**, general observations:

Compounds **1**–**6** belong to the class of  $[P_2V_3W_{15}O_{62}]^{9-}$ -based “dumb-bell” hybrid cluster anions— $[\{P_2V_3W_{15}O_{59}(OCH_2)_3CNHCO\}_2]^{12-}$ —the TBA salt of which (**7**) has been characterised by both single-crystal XRD and ESI-MS techniques.<sup>[9]</sup> The hybrid cluster in **7**, which is  $\approx 3.4$  nm long, exhibited a clear ESI-MS spectrum as shown in Figure 1. All of the major peaks in this spectrum could be assigned to the parent cluster anion  $[\{P_2V_3W_{15}O_{59}(OCH_2)_3CNHCO\}_2]^{12-}$ , with varying numbers of TBA, Na<sup>+</sup> and H<sup>+</sup> counterions. Therefore, one can expect similar structural features for the compounds **1**–**6**, to those of **7**, if their ESI-MS spectra are comparable. Dilute solutions of compounds **1**–**6** in acetonitrile with concentrations in the range of  $10^{-3}$ – $10^{-5}$  M were used for the ESI-MS analyses in the negative ion mode. Interestingly, most of these compounds gave similar spectral pattern as that of **7**, showing distinct groups of peaks corresponding to different charge states of the parent cluster anions. The detection of such a collection of multiply

charged ions of different charge states due to the attachment of different number/type of counterions is quite normal in the ESI-MS spectra of POMs.<sup>[17]</sup> As expected, the majority of the peaks in a particular group follow a isotopic distribution with a Gaussian shape, because of the presence of many tungsten atoms in compounds 1–6. One other important observation of the ESI-MS spectra of compounds 1–6 is their simplicity, probably due to the non-fragmentation of the samples under the experimental conditions in spite of their large size. Also, no major impurity peaks were observed, and this gives some indication of the purity of the samples (with respect to the presence of other intrinsically charged POM species). In all six compounds reported here, the observed experimental values are consistent, within the experimental accuracy of  $\pm 2$  in the  $m/z$  range of 1000–3500. Finally it has been observed that a number of peaks corresponding to one- or two-electron reduced species were observed in the ESI-MS spectra of most of the hybrids 1–6.

**ESI-MS analysis of “dumb-bell”-shaped hybrids 1–4:** Bis-(TRIS)-ligand-based “dumb-bell” hybrids 1–3 show similar spectral features in the mass range  $m/z \approx 1400$ –3400. Compound 1 shows three groups of peaks in the range 1600–3400 with charges of  $5^-$ ,  $4^-$  and  $3^-$ , while compounds 2 and 3 show four such groups of peaks with charges of  $6^-$ ,  $5^-$ ,  $4^-$  and  $3^-$  in the range  $m/z$  1400–3400.

Figure 2 shows the ESI-MS spectrum of compound 1 in acetonitrile. All the major peaks in the spectrum could be satisfactorily assigned to the formula  $[(P_2V_3W_{15}O_{59}(OCH_2)_3CNHCO)_2(CHOH)_2]^{12-}$  with varying combinations of TBA,  $H^+$  and  $Na^+$  counterions. For example, peaks observed at  $m/z$  values 3308.5, 2420.8 and 1931.8 correspond to  $TBA_7Na_2[(P_2V_3W_{15}O_{59}(OCH_2)_3CNHCO)_2(CHOH)_2]^{3-}$ ,  $TBA_6Na_2[(P_2V_3W_{15}O_{59}(OCH_2)_3CNHCO)_2(CHOH)_2]^{4-}$  and  $TBA_6Na[(P_2V_3W_{15}O_{59}(OCH_2)_3CNHCO)_2(CHOH)_2]^{5-}$ , re-

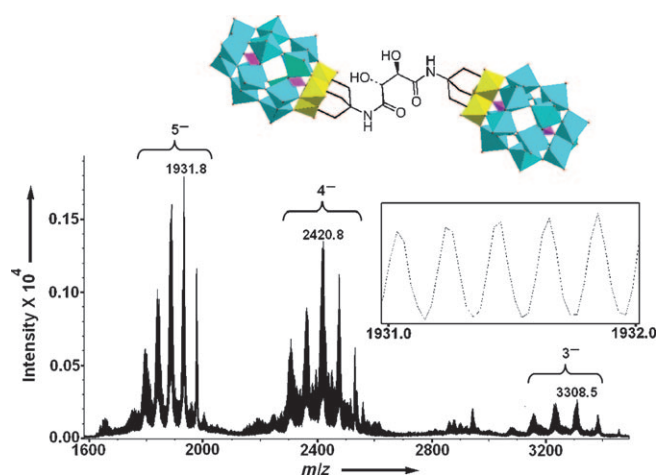


Figure 2. The molecular diagram and the negative-ion ESI mass spectrum of cluster anion in compound 1,  $[(P_2V_3W_{15}O_{59}(OCH_2)_3CNHCO)_2(CHOH)_2]^{12-}$ . The spectrum was recorded in MeCN at a concentration  $\approx 10^{-5}$  M. The inset is an expansion of the peak centred at 1931.8 to show the  $5^-$  charge state.

spectively (see Supporting Information, Figure S3a–d and Table S3 for assignment of all the peaks in the spectrum).

Figures 3 and 4 show the ESI-MS spectra of compounds 2 and 3, respectively, in acetonitrile. Since the hybrid cluster

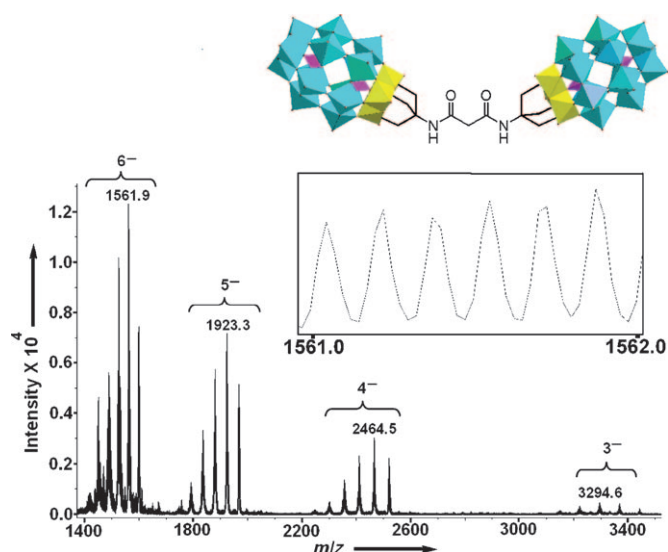


Figure 3. The molecular diagram and the negative-ion ESI mass spectrum of cluster anion in compound 2,  $[(P_2V_3W_{15}O_{59}(OCH_2)_3CNHCO)_2CH_2]^{12-}$ . The spectrum was recorded in MeCN at a concentration  $\approx 10^{-5}$  M. The inset is an expansion of the peak centred at 1561.9 to show the  $6^-$  charge state.

anions differ by only one  $-CH_2-$  unit in their organic linker chains, the ESI-MS spectra of compounds 2 and 3 are very similar in their appearance and peak positions. Unlike compound 1, these compounds exhibit four distinct groups of peaks corresponding to negatively charged species ( $6^-$ ,  $5^-$ ,  $4^-$  and  $3^-$ ) in the  $m/z$  region 1400–3500. In Figure 3, each peak represents the cluster anion  $[(P_2V_3W_{15}O_{59}(OCH_2)_3CNHCO)_2CH_2]^{12-}$ , with varying number of TBA,  $H^+$  and  $Na^+$  counterions. For example, prominent peaks observed at  $m/z$  values 3294.6, 2464.5, 1923.3 and 1561.9 correspond to  $TBA_7Na_2[(P_2V_3W_{15}O_{59}(OCH_2)_3CNHCO)_2CH_2]^{3-}$ ,  $TBA_6Na[(P_2V_3W_{15}O_{59}(OCH_2)_3CNHCO)_2CH_2]^{4-}$ ,  $TBA_6Na[(P_2V_3W_{15}O_{59}(OCH_2)_3CNHCO)_2CH_2]^{5-}$  and  $TBA_5Na[(P_2V_3W_{15}O_{59}(OCH_2)_3CNHCO)_2CH_2]^{6-}$ , respectively (see Supporting Information, Figure S4a–e and Table S4 for assignment of all the peaks in the spectrum).

Similarly, all the peaks in the spectrum of compound 3 (Figure 4) could be satisfactorily assigned to the cluster anion  $[(P_2V_3W_{15}O_{59}(OCH_2)_3CNHCO)_2(CH_2)_2]^{12-}$ . For example, peaks observed at  $m/z$  values 3296.9, 2467.9, 1925.7 and 1564.5 correspond to  $TBA_7Na_2[(P_2V_3W_{15}O_{59}(OCH_2)_3CNHCO)_2(CH_2)_2]^{3-}$ ,  $TBA_7Na[(P_2V_3W_{15}O_{59}(OCH_2)_3CNHCO)_2(CH_2)_2]^{4-}$ ,  $TBA_6Na[(P_2V_3W_{15}O_{59}(OCH_2)_3CNHCO)_2(CH_2)_2]^{5-}$  and  $TBA_5Na[(P_2V_3W_{15}O_{59}(OCH_2)_3CNHCO)_2(CH_2)_2]^{6-}$ , respectively (see Supporting Information, Figure S5a–e and Table S5 for assignment of all the peaks in the spectrum).

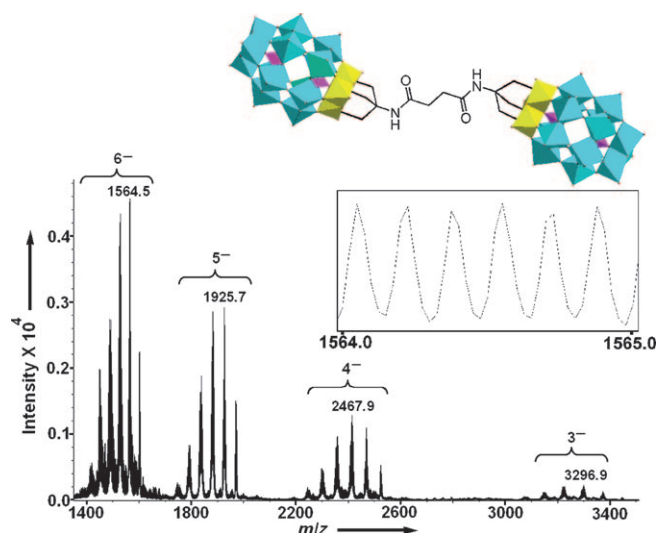


Figure 4. The molecular diagram and the negative-ion ESI mass spectrum of cluster anion in compound **3**,  $[(P_2V_3W_{15}O_{59}(OCH_2)_3CNHCO)_2-(CH_2)_2]^{12-}$ . The spectrum was recorded in MeCN at a concentration  $\approx 10^{-5}$  M. The inset is an expansion of the peak centred at 1564.5 to show the  $6^-$  charge state.

“Dumb-bell” hybrid **4**, containing a bipyridyl moiety in the linker unit, exhibits a different spectral pattern compared to compounds **1–3**. This compound exhibits a clear spectrum in the  $m/z$  range  $\approx 1700–2700$  showing two different groups of peaks corresponding to  $5^-$  and  $4^-$  charge states of the parent cluster anion. All of the peaks in these groups could be satisfactorily assigned to the formula  $[(P_2V_3W_{15}O_{59}(OCH_2)_3CNHCO)_2(C_5H_3N)_2]^{12-}$  with various combinations of TBA,  $H^+$  and  $Na^+$  counter ions, see Figure 5. Peaks observed at  $m/z$  2554.4 and 1994.3 correspond to  $TBA_8[(P_2V_3W_{15}O_{59}(OCH_2)_3CNHCO)_2(C_5H_3N)_2]^{4-}$  and  $TBA_7[(P_2V_3W_{15}O_{59}(OCH_2)_3CNHCO)_2(C_5H_3N)_2]^{5-}$ , respectively (see Supporting Information, Figure S6a–c and Table S6 for assignment of all the peaks in the spectrum).

On comparing the ESI-MS spectra of “dumb-bell” hybrids **1–4**, one could observe slight differences in their spectral features such as peak shape, position, charge states and so forth. The major reason for these observed differences is the presence/absence of different functionalities such as alcohol, bipyridyl and so forth on their bis(TRIS) linker ligands, and of course each set of compounds can be precisely modelled using an isotopic molecular-weight calculator. Our detailed studies have also shown that the differences in the nature of the organic linker units can also affect the self-assembly behaviour of  $[P_2V_3W_{15}O_{62}]^{9-}$ -based “dumb-bell” hybrids in solution.<sup>[19]</sup> However, despite the small differences in spectral features, the ESI-MS technique was highly successful in characterising these huge “dumb-bell” hybrids **1–4** unambiguously.

**ESI-MS analysis of “triangular” hybrids 5 and 6:** Tris-(TRIS)-ligand-based “triangular” hybrids **5** and **6** not only exhibited similar spectral features to those of some of the “dumb-bell” hybrids **1–4**, but also exhibited some highly

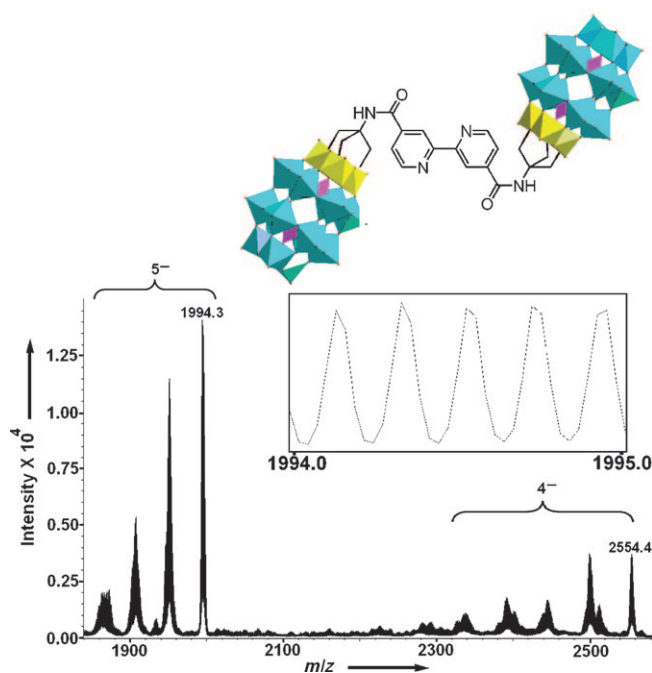


Figure 5. The molecular diagram and the negative-ion ESI mass spectrum of cluster anion in compound **4**,  $[(P_2V_3W_{15}O_{59}(OCH_2)_3CNHCO)_2-(C_5H_3N)_2]^{12-}$ . The spectrum was recorded in MeCN at a concentration  $\approx 10^{-5}$  M. The inset is an expansion of the peak centred at 1994.3 to show the  $5^-$  charge state.

charged species such as  $8^-$  and  $7^-$  as major peaks in their ESI-MS spectra. These two compounds showed four groups of peaks in the  $m/z$  range  $\approx 1700–3200$  corresponding to  $8^-$ ,  $7^-$ ,  $6^-$  and  $5^-$  charge states of the respective cluster anions. The ESI-MS spectrum of compound **5** in acetonitrile is shown in Figure 6. Almost all the peaks in this spectrum could be assigned to the formula  $[(P_2V_3W_{15}O_{59}(OCH_2)_3CNHCO)_3(C_6H_3)]^{18-}$ , with a varying number of TBA,  $H^+$  and  $Na^+$  counterions. Examples being the peaks observed at  $m/z$  values 3042.3, 2495.2, 2104.6 and 1773.5 corresponding to  $TBA_{12}Na_2[(P_2V_3W_{15}O_{59}(OCH_2)_3CNHCO)_3(C_6H_3)]^{5-}$ ,  $TBA_{11}Na_2[(P_2V_3W_{15}O_{59}(OCH_2)_3CNHCO)_3(C_6H_3)]^{6-}$ ,  $TBA_{10}Na_2[(P_2V_3W_{15}O_{59}(OCH_2)_3CNHCO)_3(C_6H_3)]^{7-}$  and  $TBA_8H_2[(P_2V_3W_{15}O_{59}(OCH_2)_3CNHCO)_3(C_6H_3)]^{8-}$ , respectively (see Supporting Information, Figure S7a–e and Table S7 for assignment of all the peaks in the spectrum).

The ESI-MS spectrum of compound **6** in acetonitrile is shown in Figure 7. The peaks could be satisfactorily assigned to the  $[(P_2V_3W_{15}O_{59}(OCH_2)_3CNHCO)_3(C_3N_3)]^{18-}$  cluster ion with varying combinations of TBA,  $H^+$  and  $Na^+$  counterions. Prominent peaks observed at  $m/z$  values 3043.3, 2452.8, 2062.2 and 1774.9 correspond to  $TBA_{12}Na_2[(P_2V_3W_{15}O_{59}(OCH_2)_3CNHCO)_3(C_3N_3)]^{5-}$ ,  $TBA_{10}NaH[(P_2V_3W_{15}O_{59}(OCH_2)_3CNHCO)_3(C_3N_3)]^{6-}$ ,  $TBA_9H_2[(P_2V_3W_{15}O_{59}(OCH_2)_3CNHCO)_3(C_3N_3)]^{7-}$  and  $TBA_8H_2[(P_2V_3W_{15}O_{59}(OCH_2)_3CNHCO)_3(C_3N_3)]^{8-}$ , respectively (see Supporting Information, Figure S8a–e and Table S8 for assignment of all the peaks in the spectrum).

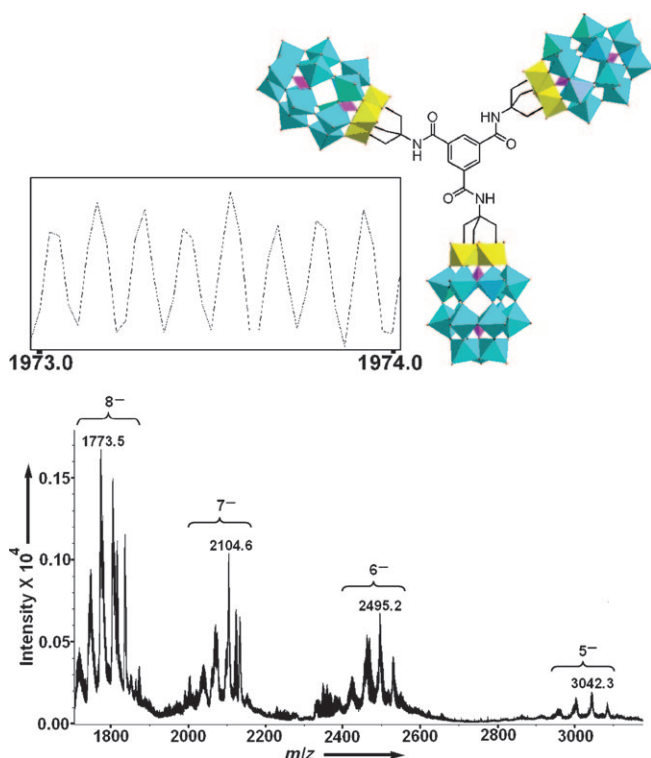


Figure 6. The molecular diagram and the negative-ion ESI mass spectrum of cluster anion in compound **5**,  $[(P_2V_3W_{15}O_{59}(OCH_2)_3CNHCO)_3-(C_6H_3)]^{18-}$ . The spectrum was recorded in MeCN at a concentration  $\approx 10^{-5}$  M. The inset is an expansion of the peak centred at 1773.5 to show the  $8^-$  charge state.

As mentioned earlier, the overall appearance of the spectra of “triangular” hybrids **5** and **6** is quite comparable to that of some of the “dumb-bell” hybrids **1–4**. However, one major difference between the spectra of both these classes of hybrids is the presence of some higher charged species such as  $8^-$  and  $7^-$  in the spectra of hybrids **5** and **6**. One possible reason for this could be the inherently high charge state of the cluster anions ( $18^-$ ) in **5** and **6** due to the presence of three  $[P_2V_3W_{15}O_{62}]^{9-}$  clusters in them.

## Conclusion

A series of tris(hydroxymethyl)aminomethane (TRIS)-based linear (bis(TRIS)) and triangular (tris(TRIS)) polyol ligands has been synthesised and were successfully grafted on to Wells–Dawson type cluster,  $[P_2V_3W_{15}O_{62}]^{9-}$  to generate a series of nanometer-sized inorganic–organic hybrid polyoxometalate clusters. These hybrids containing two or three  $[P_2V_3W_{15}O_{62}]^{9-}$  cluster units are complementary to the previous reports of similar hybrids containing one, two and four such cluster units. The synthesis of these hybrids shows that a large amount of structural design is possible in the synthesis of covalently functionalised hybrid POM clusters. High-resolution ESI-MS spectrometry was successfully employed for the unambiguous characterisation of these nanometer-sized hybrids, that have masses of the order of 10–16 kDa.

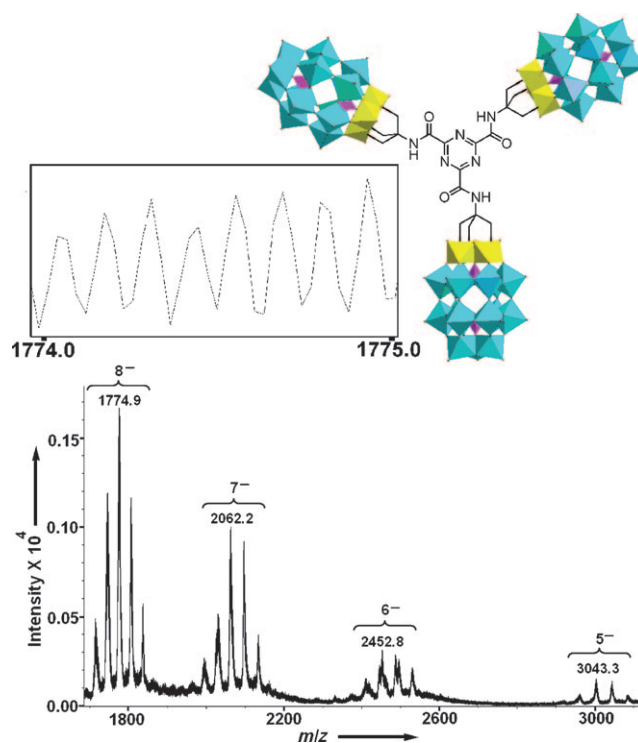


Figure 7. The molecular diagram and the negative-ion ESI mass spectrum of cluster anion in compound **6**,  $[(P_2V_3W_{15}O_{59}(OCH_2)_3CNHCO)_3-(C_3N_3)]^{18-}$ . The spectrum was recorded in MeCN at a concentration  $\approx 10^{-5}$  M. The inset is an expansion of the peak centred at 1774.9 to show the  $8^-$  charge state.

The ESI-MS spectra of the majority of these compounds in the negative ion mode were clean without excessive fragmentation peaks, and the samples tend to exhibit groups of peaks corresponding to different anionic charge states of the hybrid cluster anions, ranging from  $3^-$  to  $8^-$ . This study therefore shows that ESI-MS is a reliable technique for the characterisation of huge nanometer-sized hybrid clusters with relatively large masses. In further work we will present new types of functional hybrids that exploit the design and characterisation approach described here, in addition to studies on the self-assembly and amphiphilic surfactant properties in solution.

## Experimental Section

**General:** All reagents and chemicals including deuterated solvents were purchased from Aldrich-Sigma Company and were used without further purification. NMR spectra were recorded on a Bruker DPX 400 spectrometer at room temperature (University of Glasgow). Elemental Analyses were completed by using an Elemental Analyser MOD 1106 at University of Glasgow. IR spectra were measured using a JASCO FTIR 410 spectrometer. ESI-MS measurements were carried out at  $180^\circ\text{C}$ . The solutions of the samples were diluted so that the maximum concentration of the cluster ions was of the order of  $10^{-5}$  M, and these were infused at a flow rate of  $180\ \mu\text{L h}^{-1}$ . The mass spectrometer used for the measurements was Bruker micro TOF-Q, and the data were collected in negative mode. The spectrometer was previously calibrated with the standard tune mix to give a precision of about 1.5 ppm in the region of 500–5000 *m/z*.

The standard parameters for a medium mass data acquisition were used. Typical working conditions: the end plate voltage was set to  $-500$  V and the capillary to  $+4500$  V; the collision cell was set to collision energy  $-8.0$  eV $z^{-1}$  with a maximum gas flow rate of  $4.0$  Lh $^{-1}$ . Acetonitrile (Merck) containing the electrolyte Bu $_4$ NBF $_4$  (Fluka of Puriss Grade) was used for all voltammetric studies. Solutions used for electrochemical studies were degassed with argon for at least 10 min to remove dioxygen. Electrochemical experiments were undertaken at  $(19 \pm 1)$  °C with a Model Versastat 4 electro analysis system by Princeton Applied Research using a standard three-electrode configuration. The working electrode used for cyclic voltammetry was glassy carbon (1.5 mm diameter, BAS). The auxiliary electrode was a Pt mesh. The reference electrode consisted of a silver wire dipped into CH $_3$ CN (electrolyte) but separated from the test solution by a porous frit. The glassy carbon working electrode was polished with alumina (3  $\mu$ m) on polishing pads, rinsed with distilled water and sonicated in acetone solution before each experiment.

**Synthesis of ligands:** Ligands **L** $^1$ , **L** $^2$  and **L** $^3$  were synthesised according to published procedures.<sup>[24,25]</sup> **L** $^5$  was synthesised using synthetic procedure similar to that of **L** $^1$ –**L** $^3$  by refluxing triethyl 1,3,5-benzenetricarboxylate (294 mg, 1 mmol) with tris(hydroxymethyl)aminomethane (363 mg, 3 mmol) in methanol (40 mL) for 6 days. The desired product, which came out of the mother liquor as a white precipitate, was collected by filtering the mother liquor while hot and recrystallised from a mixture of EtOH/H $_2$ O. Yield: 0.2 g, 38%. The formation of the product was confirmed by comparing the analytical data with the literature report.<sup>[28]</sup>

**Synthesis of L** $^2$ : Diethyl 2,2'-bipyridine-4,4'-dicarboxylate was prepared according to the published procedures.<sup>[29]</sup> A mixture of diethyl 2, 2'-bipyridine-4, 4'-dicarboxylate (0.15 g, 0.5 mmol) and (HOCH $_2$ ) $_3$ CNH $_2$  (0.18 g, 1.5 mmol) in methanol (50 mL) was refluxed for 48 h. A white precipitate was isolated by filtration from hot solution and dried under vacuum. Yield 0.10 g (0.22 mmol, 44%); m. p. 144–145 °C;  $^1$ H NMR (400 MHz, [D $_6$ ]DMSO):  $\delta$  = 3.74 (d,  $J$  = 5.6 Hz, 12H; -CH $_2$ OH), 4.73 (t,  $J$  = 5.6 Hz, 6H; -OH), 7.72 (s, 2H; -NH-), 7.80 (d,  $J$  = 8.4 Hz, 2H; Ar-H), 8.73 (s, 2H; Ar-H), 8.86 ppm (d,  $J$  = 8.4 Hz, 2H; Ar-H); IR (KBr, 400–4000 cm $^{-1}$ ):  $\tilde{\nu}$  = 3289 (s), 2940 (m), 1645 (m), 1590 (w), 1550 (m), 1461 (m), 1397 (w), 1364 (w), 1308 (w), 1288 (w), 1243 (w), 1041 (s), 1022 (s), 874 (w), 788 (w), 754 (w), 701 (w), 629 cm $^{-1}$  (m); elemental analysis calcd (%) for C $_{20}$ H $_{26}$ N $_4$ O $_8$ : C 53.33, H 5.82, N 12.44; found: C 53.40, H 5.84, N 12.53.

**Synthesis of L** $^6$ : Ligand **L** $^6$  was synthesised by using a synthetic procedure similar to that used for **L** $^5$  by refluxing triethyl 1,3,5-triazine-2,4,6-tricarboxylate (297 mg, 1 mmol) with tris(hydroxymethyl)aminomethane (363 mg, 3 mmol) in methanol (40 mL) for 3 days. The desired product, which came out of the mother liquor as a white precipitate, was collected by filtering the mother liquor while hot and recrystallised from a mixture of EtOH/H $_2$ O. Yield: 0.31 g (59%).  $^1$ H NMR (400 MHz, [D $_6$ ]DMSO):  $\delta$  = 3.74 (d,  $J$  = 5.6 Hz, 12H; -CH $_2$ OH), 4.86 (t,  $J$  = 5.6 Hz, 6H; -OH), 8.39 ppm (s, 3H; -NH-); IR (KBr):  $\tilde{\nu}$  = 3344.6 (m), 2947.3 (w), 2889.4 (w), 1681.9 (s), 1523.8 (s), 1465.9 (m), 1419.6 (m), 1357.9 (m), 1253.7 (m), 1114.8 (m), 1037.74(s), 1014.5 (s), 891.1 (w), 798.5 (w), 744.5 (m), 628.8 (s) cm $^{-1}$ ; elemental analysis calcd (%) for C $_{18}$ H $_{30}$ N $_6$ O $_6$ : C 41.38, H 5.79, N 16.09; found: C 40.91, H 5.80, N 15.95.

#### Synthesis of hybrid POMs

**Synthesis of I:** TBA $_3$ H $_4$ [P $_2$ V $_3$ W $_{15}$ O $_{62}$ ]<sup>[30]</sup> (1.0 g, 0.2 mmol) was dissolved in MeCN (30 mL), then **L** $^1$  (0.030 g, 0.1 mmol) was added to the solution. The reaction mixture was heated to reflux for 6 days in dark. The resulting yellow solution was added drop-wise to excess of diethyl ether with vigorous stirring. The resulting yellow solid was collected and re-dissolved in minimum volume of MeCN, then re-precipitated by adding dropwise to excess of diethyl ether. The yellow precipitate thus obtained was isolated by filtration and recrystallised from acetonitrile by ether diffusion. Yield 0.92 g (0.09 mmol, 89%, based on TBA $_3$ H $_4$ [P $_2$ V $_3$ W $_{15}$ O $_{62}$ ]);  $^1$ H NMR (400 MHz, CD $_3$ CN):  $\delta$  = 4.07 (d,  $J$  = 6 Hz, 2H), 4.38 (d,  $J$  = 6 Hz, 2H), 5.78 (s, 12H; -CH $_2$ -), 6.82 ppm (s, 2H; -NH-) in addition to the TBA resonances; FT-IR (KBr):  $\tilde{\nu}$  = 3356.2 (w), 2962.7 (w), 2935.7 (w), 2874.0 (w), 1662.6 (m), 1462.09 (m), 1381.0 (w), 1084.0 (s), 949.0 (s), 902.7 (s), 790.84 (s), 709.83 cm $^{-1}$  (s); elemental analysis calcd (%) for

C $_{172}$ H $_{380}$ N $_{12}$ O $_{128}$ P $_4$ V $_6$ W $_{30}$ : C 19.47, H 3.61, N 1.58; found: C 19.66, H 3.77, N 1.60.

**Synthesis of 2:** The synthetic procedure was the same as that used for **1** except that **L** $^2$  was used instead of **L** $^1$ . Yield 0.94 g (0.09 mmol, 92%, based on TBA $_3$ H $_4$ [P $_2$ V $_3$ W $_{15}$ O $_{62}$ ]);  $^1$ H NMR (400 MHz, CD $_3$ CN):  $\delta$  = 3.129 (s, 2H; CH $_2$ C), 5.72 (s, 12H; -CH $_2$ O), 6.87 ppm (s, 2H; NH), in addition to the TBA resonances; FT-IR (KBr):  $\tilde{\nu}$  = 3452.7 (w), 2962.7 (m), 2935.7 (m), 2874.0 (m), 1631.8 (w), 1562.3 (w), 1465.9(m), 1381.0 (w), 1084.0 (s), 949.0 (s), 902.7 (s), 790.8 (s), 717.5 cm $^{-1}$  (s); elemental analysis calcd (%) for C $_{171}$ H $_{378}$ N $_{12}$ O $_{126}$ P $_4$ V $_6$ W $_{30}$ : C 19.44, H 3.61, N 1.59; found: C 19.24, H 3.65, N 1.55.

**Synthesis of 3:** The synthetic procedure was the same as that used for **1** except that **L** $^3$  was used instead of **L** $^1$ . Yield 0.92 g (0.09 mmol, 90%, based on TBA $_3$ H $_4$ [P $_2$ V $_3$ W $_{15}$ O $_{62}$ ]);  $^1$ H NMR (400 MHz, CD $_3$ CN):  $\delta$  = 6.31 (s, 2H; NH), 5.72 (s, 12H; -CH $_2$ O), 2.43 ppm (s, 4H; -CH $_2$ -CO-), in addition to the TBA resonances. FT-IR:  $\tilde{\nu}$  = 3452.7 (w), 2958.9 (m), 2931.9 (m), 2874.0 (m), 1678.1 (w), 1608.6 (m), 1462.0 (m), 1377.2 (w), 1157.3 (w), 1084.0 (s), 949.0 (s), 902.7 (s), 790.8 (s), 709.8 cm $^{-1}$  (s); elemental analysis calcd (%) for C $_{172}$ H $_{380}$ N $_{12}$ O $_{126}$ P $_4$ V $_6$ W $_{30}$ : C 19.53, H 3.62, N 1.59; found: C 19.51, H 3.64, N 1.56.

**Synthesis of 4:** The synthetic procedure was the same as that used for **1** except that **L** $^4$  was used instead of **L** $^1$  and the solution was heated to reflux for 9 days. The yellow precipitate was isolated by filtration and dried overnight under vacuum. Yield 0.95 g (0.09 mmol, 91%, based on TBA $_3$ H $_4$ [P $_2$ V $_3$ W $_{15}$ O $_{62}$ ]);  $^1$ H NMR (400 MHz, CD $_3$ CN):  $\delta$  = 9.16 (d,  $J$  = 8.4 Hz, 2H; Ar), 8.52 (m, 2H; Ar), 8.42 (d,  $J$  = 8.4 Hz, 2H; Ar), 7.10 (s, 2H; NH), 5.89 ppm (s, 12H; -CH $_2$ O), in addition to the TBA resonances; FT-IR (KBr):  $\tilde{\nu}$  = 3423 (w), 2961 (m), 2933 (m), 2877 (m), 1655 (w), 1557 (w), 1544 (m), 1482 (m), 1379 (w), 1086 (s), 953 (s), 913 (s), 813 (s), 735 (s), 528 (w), 471 cm $^{-1}$  (w); elemental analysis calcd (%) for C $_{180}$ H $_{382}$ N $_{14}$ O $_{126}$ P $_4$ V $_6$ W $_{30}$ : C 20.20, H 3.60, N 1.83; found: C 20.00, H 3.55, N 2.13.

**Synthesis of 5:** The synthetic procedure was the same as that used for **1** except that **L** $^5$  was used instead of **L** $^1$  in a 1:3 mole ratio. Yield 0.95 g (0.06 mmol, 92%, based on TBA $_3$ H $_4$ [P $_2$ V $_3$ W $_{15}$ O $_{62}$ ]);  $^1$ H NMR (400 MHz, CD $_3$ CN):  $\delta$  = 8.41 (s, 3H; Ar), 6.98 (s, 3H; NH), 5.91 ppm (s, 18H; -CH $_2$ O), in addition to the TBA resonances; FT-IR (KBr):  $\tilde{\nu}$  = 3348.5 (w), 2962.7 (m), 2935.7 (m), 2874.0 (m), 1662.6 (w), 1481.3(m), 1381.0(w), 1265.3 (w), 1084.0 (s), 949.0 (s), 902.7 (s), 786.9 (s), 725.2 cm $^{-1}$  (s); elemental analysis calcd (%) for C $_{261}$ H $_{567}$ N $_{18}$ O $_{189}$ P $_6$ V $_9$ W $_{45}$ : C 19.72, H 3.59, N 1.59; found: C 19.27, H 3.67, N 1.61.

**Synthesis of 6:** The synthetic procedure was the same as that used for **1** except that **L** $^6$  was used instead of **L** $^1$  in a 1:3 mole ratio. Yield 0.96 g (0.06 mmol, 93%, based on TBA $_3$ H $_4$ [P $_2$ V $_3$ W $_{15}$ O $_{62}$ ]);  $^1$ H NMR (400 MHz, CD $_3$ CN):  $\delta$  = 8.11 (s, 3H; NH), 5.92 ppm (s, 18H; -CH $_2$ O), in addition to the TBA resonances; FT-IR:  $\tilde{\nu}$  = 3464.2 (w), 2962.7 (m), 2935.7 (m), 2874.0 (m), 1631.8 (w), 1519.9 (w), 1481.3 (m), 1381.0 (w), 1084.0 (s), 949.0 (s), 902.7 (s), 790.8 (s), 725.2 cm $^{-1}$  (s); elemental analysis calcd (%) for C $_{258}$ H $_{564}$ N $_{21}$ O $_{189}$ P $_6$ V $_9$ W $_{45}$ : C 19.49, H 3.57, N 1.85; found: C 19.71, H 3.68, N 1.92.

## Acknowledgements

We thank the EPSRC, WestCHEM and the China Scholarship Council for supporting this work. We also thank Bruker Daltonics for collaboration using the microTOFQ. L.C. thanks the Royal Society and Wolfson foundation for a merit award. H.M. thanks the Royal Society of Edinburgh and Marie Curie actions for the financial support.

- [1] D.-L. Long, R. Tsunashima, L. Cronin, *Angew. Chem.* **2010**, *122*, 1780–1803; *Angew. Chem. Int. Ed.* **2010**, *49*, 1736–1758; D.-L. Long, E. Burkholder, L. Cronin, *Chem. Soc. Rev.* **2007**, *36*, 105–121; S. G. Mitchell, C. Streb, H. N. Miras, T. Boyd, D.-L. Long, L. Cronin, *Nature Chem.* **2010**, *2*, 308–312.

- [2] M. T. Pope, A. Müller, *Angew. Chem.* **1991**, *103*, 56–70; *Angew. Chem. Int. Ed. Engl.* **1991**, *30*, 34–48; *Polyoxometalate Chemistry: From Topology via Self-Assembly to Applications* (Eds.: M. T. Pope, A. Müller), Kluwer Academic, Dordrecht, **2001**; Special Issue on Polyoxometalates: *Chem. Rev.* **1998**, *98*, Issue 1.
- [3] A. Proust, R. Thouvenot, P. Gouzerh, *Chem. Commun.* **2008**, 1837–1852.
- [4] L. Xu, M. Lu, B. Xu, Y. Wei, Z. Peng, D. R. Powell, *Angew. Chem.* **2002**, *114*, 4303–4306; *Angew. Chem. Int. Ed.* **2002**, *41*, 4129–4132; Y.-F. Song, H. Abbas, C. Ritchie, N. McMillan, D.-L. Long, N. Gadegaard, L. Cronin, *J. Mater. Chem.* **2007**, *17*, 1903–1908; Y.-F. Song, N. McMillan, D.-L. Long, J. Thiel, Y. Ding, H. Chen, N. Gadegaard, L. Cronin, *Chem. Eur. J.* **2008**, *14*, 2349–2354; C. Boglio, K. Micoine, E. Derat, R. Thouvenot, B. Hasenknopf, S. Thorimbert, E. Lacôte, M. Malacria, *J. Am. Chem. Soc.* **2008**, *130*, 4553–4561.
- [5] M. Lu, Y. Wei, B. Xu, C. F. Cheung, Z. Peng, D. R. Powell, *Angew. Chem.* **2002**, *114*, 1636–1638; *Angew. Chem. Int. Ed.* **2002**, *41*, 1566–1568; Z. Peng, *Angew. Chem.* **2004**, *116*, 948–953; *Angew. Chem. Int. Ed.* **2004**, *43*, 930–935; J. L. Stark, A. L. Rheingold, E. A. Maatta, *J. Chem. Soc. Chem. Commun.* **1995**, 1165–1166.
- [6] A. Mazeaud, N. Ammari, F. Robert, R. Thouvenot, *Angew. Chem.* **1996**, *108*, 2089–2091; *Angew. Chem. Int. Ed. Engl.* **1996**, *35*, 1961–1964; F. Xin, M. T. Pope, *Organometallics* **1994**, *13*, 4881–4886; U. Kortz, F. Hussain, M. Riecke, *Angew. Chem.* **2005**, *117*, 3839–3843; *Angew. Chem. Int. Ed.* **2005**, *44*, 3773–3777; G. Sazani, M. T. Pope, *Dalton Trans.* **2004**, 1989–1994; B. Xu, Y. Wei, C. L. Barnes, Z. Peng, *Angew. Chem.* **2001**, *113*, 2353–2356; *Angew. Chem. Int. Ed.* **2001**, *40*, 2290–2292; J. B. Strong, R. Ostrander, A. L. Rheingold, E. A. Maatta, *J. Am. Chem. Soc.* **1994**, *116*, 3601–3602; J. L. Stark, V. G. Young, E. A. Maatta, *Angew. Chem.* **1995**, *107*, 2751–2753; *Angew. Chem. Int. Ed. Engl.* **1995**, *34*, 2547–2548; J. C. Duhacek, D. C. Duncan, *Inorg. Chem.* **2007**, *46*, 7253–7255; G. S. Kim, K. S. Hagen, C. L. Hill, *Inorg. Chem.* **1992**, *31*, 5316–5324.
- [7] Y. Hou, C. L. Hill, *J. Am. Chem. Soc.* **1993**, *115*, 11823–11830; H. D. Zeng, G. R. Newkome, C. L. Hill, *Angew. Chem.* **2000**, *112*, 1841–1844; *Angew. Chem. Int. Ed.* **2000**, *39*, 1771–1774.
- [8] C. P. Pradeep, D.-L. Long, G. N. Newton, Y.-F. Song, L. Cronin, *Angew. Chem.* **2008**, *120*, 4460–4463; *Angew. Chem. Int. Ed.* **2008**, *47*, 4388–4391.
- [9] C. P. Pradeep, M. F. Misdrabi, F.-Y. Li, J. Zhang, L. Xu, D.-L. Long, T. Liu, L. Cronin, *Angew. Chem.* **2009**, *121*, 8459–8463; *Angew. Chem. Int. Ed.* **2009**, *48*, 8309–8313.
- [10] J. Li, I. Huth, L.-M. Chamoreau, B. Hasenknopf, E. Lacôte, S. Thorimbert, M. Malacria, *Angew. Chem.* **2009**, *121*, 2069–2072; *Angew. Chem. Int. Ed.* **2009**, *48*, 2035–2038.
- [11] Y. Han, Y. Xiao, B. Liu, P. Zheng, S. He, W. Wang, *Macromolecules* **2009**, *42*, 6543–6548.
- [12] J. R. Morgan, M. J. Cloninger, *J. Polym. Sci. Part A: Polym. Chem.* **2005**, *43*, 3059–3066.
- [13] M. Góral, T. McCormac, E. Dempsey, D.-L. Long, L. Cronin, A. M. Bond, *Dalton Trans.* **2009**, 6727–6735.
- [14] Z. Luo, P. Kögerler, R. Cao, C. L. Hill, *Inorg. Chem.* **2009**, *48*, 7812–7817.
- [15] J. B. Fenn, M. Mann, C. K. Meng, S. F. Wong, C. M. Whitehouse, *Science* **1989**, *246*, 64–71; P. Kebarle, U. H. Verkerk, *Mass Spectrom. Rev.* **2009**, *28*, 898–917; R. D. Smith, J. A. Loo, C. G. Edmonds, C. J. Barinaga, H. R. Udseth, *Anal. Chem.* **1990**, *62*, 882–899; R. D. Voyksner, *Nature* **1992**, *356*, 86–87.
- [16] H. N. Miras, E. F. Wilson, L. Cronin, *Chem. Commun.* **2009**, 1297–1311.
- [17] T. C. Lau, J. Wang, K. W. M. Siu, R. Guevremont, *J. Chem. Soc. Chem. Commun.* **1994**, 1487–1488; J. Le Quan Tuoi, E. Muller, *Rapid Commun. Mass Spectrom.* **1994**, *8*, 692–694; T. C. Lau, J. Wang, R. Guevremont, K. W. M. Siu, *J. Chem. Soc. Chem. Commun.* **1995**, 877–878; M. J. Deery, O. W. Howarth, K. R. Jennings, *J. Chem. Soc. Dalton Trans.* **1997**, 4783–4788; C. Dablemont, A. Proust, R. Thouvenot, C. Afonso, F. Fournier, J.-C. Tabet, *Inorg. Chem.* **2004**, *43*, 3514–3520; C. R. Mayer, M. Hervé, H. Lavanant, J.-C. Blais, F. Sécheresse, *Eur. J. Inorg. Chem.* **2004**, 973–977; C. R. Mayer, C. Roch-marchal, H. Lavanant, R. Thouvenot, N. Sellier, J.-C. Blais, F. Sécheresse, *Chem. Eur. J.* **2004**, *10*, 5517–5523.
- [18] E. F. Wilson, H. Abbas, B. J. Duncombe, C. Streb, D.-L. Long, L. Cronin, *J. Am. Chem. Soc.* **2008**, *130*, 13876–13884; D.-L. Long, Y.-F. Song, E. F. Wilson, P. Kögerler, S.-X. Guo, A. M. Bond, J. S. J. Hargreaves, L. Cronin, *Angew. Chem.* **2008**, *120*, 4456–4459; *Angew. Chem. Int. Ed.* **2008**, *47*, 4384–4387; J. Yan, D.-L. Long, H. N. Miras, L. Cronin, *Inorg. Chem.* **2010**, *49*, 1819–1825; E. F. Wilson, H. N. Miras, M. H. Rosnes, L. Cronin, *Angew. Chem.* **2011**, *123*, 3804–3808; *Angew. Chem. Int. Ed.* **2011**, *50*, 3720–3724.
- [19] M. F. Misdrabi, M. Wang, C. P. Pradeep, F.-Y. Li, C. Lydon, L. Xu, L. Cronin, T. Liu, unpublished results.
- [20] J. W. Han, C. L. Hill, *J. Am. Chem. Soc.* **2007**, *129*, 15094–15095.
- [21] S. Favette, B. Hasenknopf, J. Vaissermann, P. Gouzerh, C. Roux, *Chem. Commun.* **2003**, 2664–2665; B. Hasenknopf, R. Delmont, P. Herson, P. Gouzerh, *Eur. J. Inorg. Chem.* **2002**, 1081–1087; P. R. Marcoux, B. Hasenknopf, J. Vaissermann, P. Gouzerh, *Eur. J. Inorg. Chem.* **2003**, 2406–2412; C. Allain, S. Favette, L.-M. Chamoreau, J. Vaissermann, L. Ruhlmann, B. Hasenknopf, *Eur. J. Inorg. Chem.* **2008**, 3433–3441.
- [22] Y.-F. Song, D.-L. Long, L. Cronin, *Angew. Chem.* **2007**, *119*, 3974–3978; *Angew. Chem. Int. Ed.* **2007**, *46*, 3900–3904; J. Zhang, Y.-F. Song, L. Cronin, T. Liu, *J. Am. Chem. Soc.* **2008**, *130*, 14408–14409.
- [23] Y.-F. Song, D.-L. Long, S. E. Kelly, L. Cronin, *Inorg. Chem.* **2008**, *47*, 9137–9139; Y.-F. Song, N. McMillan, D.-L. Long, S. Kane, J. Malm, M. O. Riehle, C. P. Pradeep, N. Gadegaard, L. Cronin, *J. Am. Chem. Soc.* **2009**, *131*, 1340–1341.
- [24] G. E. DuBois, B. Zhi, G. M. Roy, S. Y. Stevens, M. Yalpani, *J. Chem. Soc. Chem. Commun.* **1992**, 1604–1605.
- [25] C. Fernandes, J. L. Wardell, A. Horn, Jr., J. M. S. Skakle, V. Drago, *Polyhedron* **2004**, *23*, 1419–1426; C. Fernandes, J. L. Wardell, J. M. S. Skakle, *Acta Crystallogr. Sect. C* **2002**, *58*, o499–o502.
- [26] E. K. Brechin, *Chem. Commun.* **2005**, 5141–5153; A. Ferguson, A. Parkin, J. Sanchez-Benitez, K. Kamenev, W. Wernsdorfer, M. Murrie, *Chem. Commun.* **2007**, 3473–3475.
- [27] P. R. Ashton, E. F. Hounsell, N. Jayaraman, T. M. Nilsen, N. Spencer, J. F. Stoddart, M. Young, *J. Org. Chem.* **1998**, *63*, 3429–3437; P. R. Ashton, S. E. Boyd, C. L. Brown, N. Jayaraman, J. F. Stoddart, *Angew. Chem.* **1997**, *109*, 756–759; *Angew. Chem. Int. Ed. Engl.* **1997**, *36*, 732–735.
- [28] B. A. Hernandez, V. Chang, I. Villanueva, M. D. Heagy, *J. Org. Chem.* **1999**, *64*, 6905–6906.
- [29] C. Janiak, S. Deblon, H.-P. Wu, M. J. Kolm, P. Klüfers, H. Piotrowski, P. Mayer, *Eur. J. Inorg. Chem.* **1999**, 1507–1521.
- [30] R. G. Finke, B. Rapko, R. J. Saxton, P. J. Domaille, *J. Am. Chem. Soc.* **1986**, *108*, 2947–2960.

Received: January 24, 2011

Published online: May 18, 2011